Effects of overconsolidation on the reactivated residual strength of remoulded deep-seated sliding zone soil in the Three Gorges Reservoir Region, China

Yanhao Zheng[1], Matthew Richard Coop[1], Huiming Tang[2,*], Zhiqiang Fan[2,3,*]

[1] Department of Civil, Environmental and Geomatic Engineering, University College London, London WC1E 6BT, The United Kingdom

[2] Faculty of Engineering, China University of Geosciences, Wuhan, Hubei 430074, China

[3] Huadong Engineering Corporation Limited

*Corresponding author: Zhiqiang Fan

E-mail address: fan_zq@hdec.com (Zhiqiang Fan)

A manuscript submitted to *Engineering Geology* for review

Abstract

Due to the landslide-prone geological conditions, many landslides have occurred in the Three Gorges Reservoir Region (TGRR), most of which are slow-moving ancient landslides characterized by preexisting shear surfaces. In this study, with the purpose of making full use of reactivated residual strength to prevent and treat the slow-moving landslides, such as designing anti-slide piles, the Huangtupo landslide as a typical reactivated ancient landslide in the TGRR was selected to study the overconsolidation (OCR) effect on the reactivated residual strength of deep-seated sliding zone soil by conducting a series of laboratory ring shear tests. It was found that after a short rest of one day, the reactivated residual strength increased with the increase of OCR under a given normal effective stress, but it was lost after a small shear displacement. The overconsolidation effect on reactivated residual strength at a lower stress was more prominent than that at a higher stress. Very coarse sand with a size of 1-2 mm inside the remoulded deep-seated sliding zone soil sample exerts direct control on the reactivated residual strength, and it significantly influences the overconsolidation effect on reactivated residual strength. The results could provide a reliable scientific basis for improving the stability analysis and reinforcement measures of the slow-moving landslides in the TGRR, as well as can be applied to similar slow-moving landslides in other areas.

Key words: Reactivated residual strength; Overconsolidation; Ring shear; Deep-seated sliding zone soil

1. Introduction

Large-scale landslides have become a typical geological disaster in reservoir areas because of the seasonal rainfall and periodic fluctuation of reservoir water level (Serafim, 1987; Kilburn and Petley, 2003; Tan et al., 2018; Dai et al., 2022; Zhou et al., 2022). As the largest reservoir in China, the Three Gorges Reservoir has become a typical landslide-prone area. It is documented that more than 4200 landslides had occurred in the Three Gorges Reservoir Region (TGRR) by 2017 (Li et al., 2017), and this number is still on the rise (Li et al., 2019; Wang et al., 2020). Most of the landslides in the TGRR were ancient landslides, and they were activated as slow-moving landslides mainly because the reservoir impoundment would fluctuate the TGRR's hydrologic conditions (Miao et al., 2014; Huang et al., 2018; Song et al., 2018; Liao et al., 2022; Wang et al., 2022). These slow-moving landslides are characterized by relatively small displacements and large-scale mass movement (Wang et al., 2020), which have caused extensive damage to nearby infrastructure and posed a significant threat to the residents.

The reactivated landslide typically has a sudden and quick displacement at the beginning, after which it tends to stabilize at low translational velocity, finally forming a new quiescence cycle (Carrubba and Del Fabbro, 2008; Kundu and Gupta, 2022). Reactivation of a quiescent landslide is a phenomenon induced by natural causes and human activities, before which a temporarily available strength along the preexisting sliding surface inside the landslide has been generated from the residual state of shear during a quiescence period. It has been well documented that this mobilized available strength is always greater than previous residual strength (e.g., Ramiah et al., 1973; Skempton, 1985; Stark et al., 2005; Ren et al., 2021; Sanshao et al., 2021). Here the recovered residual shear strength at reactivation is referred to as reactivated residual strength.

Over the past several decades, many studies have been carried out on the reactivated residual strength. D'Appolonia et al. (1967) first proposed the self-healing effect that the reactivated residual strength was greater than the drained residual strength for an ancient landslide. Carrubba and Del Fabbro (2008) explained the healing phenomenon by the fact that the skeleton structure of soil particles became more stable over time through some processes, such as creep and thixotropic hardening. Since the residual strength is reactivated and increased after a period of quiescence, many research works have focused on the time effect on the reactivated residual strength of different soils, including remoulded kaolinite and bentonite for a rest period of 4 days (Ramiah et al., 1973), montmorillonitic clays for different rest times up to 5 days (Angeli et al., 1996), remoulded smectite-dominant landslide soils for a short rest duration of 2 days (Gibo et al., 2002), and low-plasticity Duck Creek shale and high-plasticity Otay bentonitic shale for two ageing times, 1 day and 230 days, respectively (Stark et al., 2005). The common conclusion from these studies is that the magnitude of strength gain increases with time, even over a short rest period of time. In addition to the time effect, Bellino and Maugeri (1985) pointed out that the reactivated residual strength depended on the shear apparatus by testing the identical soil sample with two different types of ring shear apparatus. Skempton (1985) and Lemos (2003) also demonstrated that the shearing rate had a significant influence on reactivated residual strength due to the viscous properties of clay soils.

However, the effects of overconsolidation ratio (OCR) on the reactivated residual strength have not yet been reported in the geotechnical literature. Most of the research has focused on the effects of loading and unloading normal stress on the residual shear strength of slip soils because residual strength can be used to design and repair the reactivated landslides with the preexisting shear surface. For example, Vithana et al.(2012) demonstrated that the residual strength of a high plasticity slip soil was independent of stress history through drained torsional ring shear tests, which is consistent with the findings of Bishop et al. (1971), Townsend and Gilbert (1976), and Stark et al. (2005). However, compared to residual strength, reactivated residual strength should be better utilized in the stability analysis and treatment of reactivated landslides. More importantly, in the TGRR, the fast infiltration of seasonal rainfall and the fluctuation of water level make the shallow soil easy to be saturated, thereby triggering a huge number of common shallow landslides (Miao et al., 2014). In this way, the original overconsolidation state of the soil in the deep-seated sliding zone of ancient landslides will change greatly, which is highly likely to affect the reactivated residual strength of the soil.

In this backdrop, this study examines the effect of OCR on the reactivated residual strength of deep-seated sliding zone soil from the TGRR, China. A series of laboratory ring shear tests were carried out on the remoulded soil samples with different artificial overconsolidation ratios under different normal effective stresses. The main objectives of the present study are as follows: (1) to find out the OCR effect on the magnitude of soil strength gain from the residual state of shear over a short rest time; (2) to compare the OCR effect on the reactivated residual strength under different normal effective stresses; and (3) to understand the influence mechanism of OCR on the reactivated residual strength at the residual state of shear.

2. Materials

2.1. The Huangtupo landslide

The Huangtupo landslide is located along the Yangtze River in China, 69 km east of the Three Gorges Dam (Fig. 1). As a typical slow-moving ancient landslide, it is now the largest landslide ever identified in the TGRR (Tan et al., 2018). More details on the geologic setting of the Huangtupo landslide can be found in the literature (Deng et al., 2000; Tang et al., 2015b; Tang et al., 2019). The Huangtupo 1# landslide is one of four regional landslide areas in the Huangtupo landslide and has the most serious deformation (Tan et al., 2018). The geological profile of Huangtupo 1# landslide (Fig. 2) suggests that it is a chaotic mass consisting of shallow sliding mass and deep-seated sliding mass. To monitor this landslide in real time, an arc-shaped testing tunnel of 908 m long was constructed in 2010 crossing the Huangtupo 1# landslide (Tang et al., 2015a) and five branch tunnels (BT-1 to BT-5) were connected to the main tunnel, as shown by the pink line in Fig. 3. The sampling site is located at the end of BT-5 where the deep-seated sliding zone soil is exposed (Fig. 3). The deep-seated sliding zone soil here is a kind of reddish-brown fine-grained soil with a small amount of gravel.

2.2. Testing materials

The soil samples used in this study were taken from the deep-seated sliding zone of Huangtupo 1# landslide (Fig. 3). The collected undisturbed soil samples were firstly air-dried and then hand-milled with a roller to pass through the standard 2 mm sieve, following the method described by Vithana et al. (2012). The sieving of particles larger than 2 mm in size is mainly limited by the ring shear apparatus, in this way which excludes bigger gravels and soil aggregates while retaining all primary soil particles. The removed materials accounted for approximately 7.6% by weight. The remaining soil samples were used as the testing materials.

The basic geotechnical properties of the tested soil were measured in the laboratory, as listed in Table 1. The grain size distribution was determined by using dry sieve method and sedimentation by the hydrometer method following BS1377: Part 2: 1990. The grading curve (Fig.4) indicates this is a well-graded soil. The liquid limit is 30.4%, measured using the cone penetrometer method, and the plastic limit is 12.8%, determined by the standardized thread-rolling method, indicative of the low plasticity of the soil. The mineralogical composition was quantitatively identified by X-ray diffraction test (XRD) using a PANalytical X'Pert Pro diffractometer, reported in Table 2. The XRD pattern of the clay fraction (< 0.002 mm) of the soil is shown in Fig. 5, obtained by X-raying the specimen with solvating by saturated ethylene glycol.

3. Experimental details

3.1. Ring shear apparatus

In the ring shear test, the Bromhead ring shear apparatus (Bromhead, 1979), with an inner diameter of 70 mm and an outside diameter of 100 mm, was used to evaluate the residual strength. The initial thickness of the annular sample was about 5 mm. Compared to other shear tests, the ring shear test can better simulate the large one-way displacement of a landslide for its total magnitude in the laboratory (Vithana et al., 2012). The ring shear apparatus makes the soil particles be oriented parallel to the shear direction by unidirectional continuous shearing, which conforms to the actual residual shear strength condition.

3.2. Sample preparation

The remoulded state of the specimen was prepared by adding the distilled water to the air-dried sample with great care until the water content of the soil sample reached 1.5 times the liquid limit, following Carrubba and Del Fabbro (2008). Then, the remoulded soil sample was de-aired in a vacuum chamber to ensure that the sample was fully saturated when placed on the shear disc. It is noted that extra care needs to be taken when placing the soil paste into the annular cavity to avoid trapping air bubbles. The remoulded soil sample in the ring shear apparatus was always submerged in a water bath during consolidation and shearing to maintain a fully saturated state.

3.3. Overconsolidation ratio (OCR)

Before conducting ring shear tests, the overconsolidation states of remoulded soil samples (OCR=1, 2, 3, and 4) were artificially created. Note that the actual overconsolidated condition of the deep-seated sliding zone soil in the field is much greater than the OCR of 4, even one to two orders of magnitude higher. It is impossible to create such a high OCR in the laboratory, so four easily available OCRs were selected in this study, following Vithana et al. (2012). To create different OCRs of 2, 3, and 4, the annular soil samples on the Bromhead apparatus were firstly consolidated at the desired consolidation stress (See Table 3) until the samples had reached the end of primary consolidation, confirmed from the deformation-square root time curve. Next, the consolidation stress previously applied was reduced to the normal effective stress (σ'_n) required for shearing (i.e., 75 kPa or 300 kPa), and this stress remained constant during shearing. The soil samples were then reconsolidated under the required normal effective stress for a period of time until the vertical gauge was stable, after which the ring shear tests were ready to perform. For example, to achieve the consolidation state with an OCR of 4, the designed consolidation stress of 1200 kPa was first applied to the prepared remoulded sample. After the samples reached the end of primary consolidation, this consolidation stress was reduced to 300 kPa, which was the normal effective stress the sample was subjected to during shearing. When reaching the stable state again, the overconsolidated sample with an OCR of 4 was ready for the ring shear test. For the normally consolidated soil samples (OCR=1), they were consolidated directly at 75 kPa and 300 kPa without unloading.

3.4. Reactivation tests

Before the reactivation tests, a series of ring shear tests were firstly carried out on the remoulded soil samples with different OCRs at a given stress to obtain the residual state of shear and the residual strength in the fully saturated state. All the shear tests were run in drained conditions, and the excess pore water pressure was assumed to dissipate during shearing. Therefore, it is important to select an appropriate shearing rate to minimize the variation of pore water pressure induced by shearing. In this work, the soil samples were sheared at a slow constant shearing rate of 0.1 mm/min to ensure the drained conditions and avoid possible rate effects, following Carrubba and Del Fabbro (2008).

In the reactivation test, the previous shearing was firstly stopped, but the sample that had been sheared to the residual state was still placed in the Bromhead apparatus. As the sliding body is still subjected to the shear force after sliding in the field (Bhat et al., 2014), during the rest period, the soil sample was always subjected to the vertical load and the shear force applied at the end of the previous ring shear test in order to better simulate the field conditions of the landslide. With reference to the minimum rest time selected in previous studies on residual strength (e.g., Angeli et al., 1996; Angeli et al., 2004; Stark et al., 2005; Stark and Hussain, 2010; Bhat et al., 2014), one day (24 hours) was chosen as the rest time in this study for saving time. It is widely acknowledged that the reactivated residual strength increases with time (Stark et al., 2005; Carrubba and Del Fabbro, 2008; Bhat et al., 2014). If the overconsolidation effect on the reactivated residual strength can be observed within a short rest time, this effect will also exist for a long rest period. During the rest period the readings of two proving rings did not change, indicating that the shear force did not change in the creep period. This is because the proving rings used to measure load have a large stored energy. After one-day rest, the ring shear test was restarted at the shearing rate of 0.1 mm/min. The reactivated residual strength was captured and measured within a very short time after restart. Shearing then was continued until the reactivated strength decayed to the initial residual strength again with additional shear displacements. The details of all the reactivation tests are shown in Table 3.

4. Results and discussion

4.1. Effects of overconsolidation on peak strength and residual strength

Figs. 6 and 7 show the relationship between shear stress and shear displacement of remoulded soil samples at 75 kPa and 300 kPa, respectively. It is found that the peak strength (τ_p) of the overconsolidated soil samples was significantly higher than that of the normally consolidated soil samples. It should be noted that generally a normally consolidated soil should have no peak if it is sheared to the critical state (Skempton, 1970), but a peak did occur in this work, which can be explained by the fact that the normally consolidated sample was sheared to the residual state. The large gap between the residual state and the critical state highlights this peak that should not exist. As shown in Fig. 8a, the stress ratio of peak strength to normal effective stress (τ_p/σ'_n) increased linearly with the increase of OCR. Since the soil sample used in this study is in a remoulded state, the peak strength only depends on dilation (Schofield, 2006). For the soil samples with higher OCR, they had experienced larger preconsolidation pressure before, which made the soil particles in the ring become more compact with each other, resulting in greater dilation. Note that the peak strength measured by Bromhead ring shear apparatus is slightly underestimated because of progressive failure (Bromhead, 1979), but the width of the annulus is designed to be narrow enough to minimize the effect of non-uniform strain.

As observed from Figs.6 and 7, the residual strength (τ_r) was constant as OCR increased. Compared to the residual friction angle of sliding zone soils from the large landslides in the TGRR (Wen et al., 2007) and other areas (e.g., Bromhead and Dixon, 1986; Vithana et al., 2012), the residual friction angle of the tested soil is much higher, ranging from 17.7° at 300 kPa to 23.3° at 75 kPa. The peak friction angle of the normally consolidated tested soil ranges from 22.2° at 300 kPa to 26.9° at 75 kPa, indicating that the soil in this study is typical of a well-graded soil with less strain softening to the residual state. For such a well-graded soil, the mechanism controlling residual shearing should be the combination of turbulent rolling shear and sliding shear, but turbulent rolling shear is the predominant mode (Lupini et al., 1981). At 300 kPa, the shear behaviour would have a greater component of the sliding residual shear mode in which the particles on the shear surface are orientated, meaning that there will be more particle orientation (but still not be very complete) and less rolling with slightly more tendency to sliding. While at 75 kPa, the turbulent rolling shear of bulky particles dominates and the sliding mode has less impact, giving rise to higher strength (Lupini et al., 1981). Therefore, it is no surprise that the stress ratios of residual strength to normal effective stress (τ_r/σ'_n) at 300 kPa were all smaller than those at 75 kPa (See Fig. 8b). Two horizontal lines in Fig. 8b suggest that under the same stress, the overconsolidation, at least up to OCR of 4, had little effect on residual strength, which is consistent with previous findings (Bishop et al., 1971; Stark et al., 2005; Vithana et al., 2012).

4.2. Effects of overconsolidation on reactivated residual strength

In Figs. 6 and 7, a strength gain occurred after resting. The reactivated residual strength (τ_{rea}) increased with the increase of OCR, but it was lost after a small shear displacement. Following Stark and Hussain (2010), this overconsolidation effect was quantitatively evaluated by the recovery strength ratio (*RSR*), which is expressed as follows:

$$RSR = \frac{\tau_{rea} - \tau_{r}}{\tau_{p} - \tau_{r}} \times 100\% \quad (1)$$

The value of *RSR* ranges from 0 to 1 where 0 indicates that the residual strength does not recover ($\tau_{rea} = \tau_{r}$) while 1 indicates that the residual strength is reactivated to the peak strength ($\tau_{rea} = \tau_{p}$). The *RSR* for each reactivation test is plotted in Fig. 9. It can be observed that under a given stress, *RSR* shows an upward trend with the increase of OCR, corresponding to the gradual increase in reactivated residual strength in Figs. 6b and 7b. This suggests that the reactivated residual strength was affected by the stress history, i.e., overconsolidation, and the phenomenon of residual strength recovery became more obvious with increasing OCR.

Fig. 9 also shows that the values of *RSR* at 75 kPa were much greater than those at 300 kPa, which is in agreement with the previous study by Carrubba and Del Fabbro (2008) that the increase in reactivated residual strength was inversely proportional to normal stress. This could be because at a lower stress (75 kPa) during the rest period soil particles originally oriented parallel to the shear direction rebounded more easily to the state before large shear displacements (Stark and Hussain, 2010), resulting in a greater shear resistance compared to previously attained residual strength, while at a higher stress (300 kPa) the soil particles did not rebound or reorient as easily and so there was a greater alignment of particles with the direction of shear (Stark and Hussain, 2010). This speculation needs to be proved by using a scanning electron microscope to observe soil particles at 75 kPa and 300 kPa, respectively, during the rest period.

4.3. Influence of very coarse sand on overconsolidation effect

According to the USDA Soil Textural Classification System, the soil with a particle size of 1-2 mm is classified as very coarse sand. In this study, a hypothesis is proposed that the overconsolidation effect on the reactivated residual strength is largely dependent on the very coarse sand with the particle size greater than 1 mm inside the soil sample. To confirm this hypothesis, some supplementary reactivation tests were conducted at 300 kPa on the remoulded soil samples with the particles greater than 1mm removed. The test results, as illustrated in Fig. 10, show that the peak strength gradually increased with the increase of OCR, while the residual strength was not affected by overconsolidation.

According to the data in Table 4, it is found that the residual strength of soil samples with particles smaller than 1 mm (95.4 kPa) was slightly smaller than that of samples with very coarse sand (96.6 kPa), perhaps because the very coarse sand increased the shear surface roughness, thus leading to an increase of the friction resistance (Wen et al., 2007). It could also be that the very coarse sand increased the turbulent rolling component of particle motion compared to sliding.

The overconsolidation effect on the reactivated residual strength of soil samples without very coarse sand was also evaluated by *RSR*, as illustrated in Fig. 11. For soil samples with OCR of 1 and 2, the *RSR* was zero, indicating that there was no strength recovery over a short rest time of one day. As the OCR increased to 3, a very small increase in *RSR* occurred, about 1%. By continuously increasing OCR to 4, *RSR* increased to 2.9%. For soil samples with OCR of 3 or 4, the small increase of *RSR* can be explained by the rebound or reorientation of soil particles during the rest period. According to Table 4, under the same normal effective stresses of 300 kPa, for the soil sample containing very coarse sand with an OCR of 4, the *RSR* of 22.6% is nearly an order of magnitude larger than the *RSR* of 2.9% for the soil sample without coarse sand. The huge difference between the two values suggests that the very coarse sand is the dominant factor for the overconsolidation effect, even though it only accounts for about 15% by weight.

To investigate further the influence mechanism of overconsolidation on reactivated residual strength, some microscopic observations were carried out on the very coarse sand inside the soil sample. The images before shearing are shown in Fig. 12a. It can be observed that these sand particles are different in shape, but most of them have some sharp edges. At the residual state of shear, 100 particles of very coarse sand below the shear band were collected and quantitatively evaluated by a Morphologi G3 particle analyzer. Here HS (High Sensitivity) Circularity and Aspect Ratio were used to quantify the shape characteristics. HS Circularity was calculated as the square of the ratio of the perimeter of a circle with the same area as the particle divided by the perimeter of the actual particle image. Aspect Ratio was calculated as the width divided by the length, where the width and the length are, respectively, the shortest and longest possible lines of the projection between two points on the perimeter of the particle. The HS Circularity is 1 for a perfect circle and is close to 0 for a 'spiky' object. Detailed descriptions of these two parameters can be found in Fan et al. (2021). Figs. 12b and 12c show the HS Circularity and Aspect Ratio distributions of 100 particles of very coarse sand in the form of a scatter plot, respectively. The values of HS Circularity are concentrated between 0.2 and 0.5 and the values of Aspect Ratio are concentrated between 0.5 and 0.8, together indicating that the very coarse sand particles below the shear band are irregular in shape, and most of them have a protruding edge.

Consequently, a possibility for the influence mechanism of the very coarse sand on the overconsolidation effect is that during the rest period the soil samples had slow settlements (creep), which caused the very coarse sand particles below the shear band to pierce the preexisting sliding surface by their protruding edges and reduce the degree of alignment and ordered state.

5. Conclusions

This study investigated the overconsolidation effect on the reactivated residual strength of a remoulded deep-seated sliding zone soil from the TGRR, China, by conducting the ring shear tests. Based on the results of laboratory reactivation tests and the shape analysis of very coarse sand particles, the following conclusions are derived from this work:

The soil from the deep-seated sliding zone of Huangtupo 1# landslide is typical of a well-graded soil with a higher residual friction angle that is closer to the critical state with less strain softening to the residual state. For such a type of fine-grained soil, the effect of overconsolidation on peak strength was far more prominent than that on residual strength. As the OCR increased, the peak strength gradually increased linearly, but the residual strength was not affected by stress history, at least up to OCR of 4. After a short rest of one day, the reactivated residual strength increased with the increase of OCR under a given stress, but it was lost after a small shear displacement. The overconsolidation effect on reactivated residual strength at a lower stress was more prominent than that at a higher stress probably because during the rest period soil particles originally oriented parallel to the shear direction rebounded more easily towards the state before large shear displacements at a lower stress.

Very coarse sand with a size of 1-2 mm inside the remoulded soil sample was directly related to the reactivated residual strength, and the overconsolidation effect on reactivated residual strength largely depended on these coarse sands. It can be speculated that over the rest period, the very coarse sand particles below the shear band can pierce the preexisting sliding surface by their protruding edges under the action of the normal stress and break up the previous residual state of shear. However, the precise reason why the reactivated residual strength increases with the increase of OCR needs to be studied further.

Acknowledgments

M. Yanhao Zheng is grateful to the China Grants Council for the award of a full scholarship (CSC No. 201808060470) allowing him to carry out his research at UCL. All the tests in the present study were done at UCL. This study was financially supported by the National Basic Research Program Project (973 Project) of the Ministry of Science and Technology of China (Grant no. 2011CB710600).

Reference:

1. Angeli, M.G., Gasparetto, P., Menotti, R.M., Pasuto, A., Silvano, S., 1996. A visco-plastic model for slope analysis applied to a mudslide in Cortina d'Ampezzo, Italy. Quarterly Journal of Engineering Geology and Hydrogeology 29(3), 233-240.
2. Angeli, M.G., Gasparetto, P., Bromhead, E., 2004. Strength-regain mechanisms in intermittently moving slides. In Landslides: evaluation and stabilization, 689-696.
3. Bellino, S., and Maugeri, M., 1985. Confronto tra valori di resistenza residua ottenuti con diverse apparecchiature anulari di taglio. Riv. Ital. Geotec. 2, 101–114.
4. Bhat, D.R., Yatabe, R., Bhandary, N.P., 2014. Strength Recovery of Landslide Soils from the Residual State of Shear. In Soil Behavior and Geomechanics (254-264).
5. Bishop, A.W., Green, G.E., Garga, V.K., Anderson, A., Brown, J.D., 1971. A new ring shear apparatus and its application to themeasurement of residual strength. Géotechnique 21 (4), 273–328.
6. British Standards Institution, 1990 . Methods of test for soils for civil engineering purposes: BS1377, PART 2, Classification tests. British Standards Institution, London.
7. Bromhead, E.N., 1979. A simple ring shear apparatus. Ground engineering, 12(5).

8. Bromhead, E.N., Dixon, N., 1986. The field residual strength of London Clay and its correlation with loboratory measurements, especially ring shear tests. Géotechnique, 36(3), 449-452.

9. Carrubba, P., Del Fabbro, M., 2008. Laboratory investigation on reactivated residual strength. J. Geotech. Geoenviron. 134(3), 302-315.

10. D'Appolonia, E., Alperstein, R., D'Appolonia, D. J., 1967. Behaviour of a colluvial slope. J. Soil Mech. and Found. Div. 93(4), 447–473.

11. Dai, Z., Zhang, Y., Zhang, C., Luo, J., Yao, W., 2022. Interpreting the Influence of Reservoir Water Level Fluctuation on the Seepage and Stability of an Ancient Landslide in the Three Gorges Reservoir Area: A Case Study of the Outang Landslide. J. Geotech. Geoenviron., 1-11.

12. Deng, Q.L., Zhu, Z.Y., Cui, Z.Q., Wang, X.P., 2000. Mass rock creep and landsliding on the Huangtupo slope in the reservoir area of the three Gorges project, Yangtze river, China. Eng. Geol. 58 (1), 67–83.

13. Fan, K., Zheng, Y., Baudet, B.A., Cheng, Y.P.H., 2021. Investigation of the ultimate particle size distribution of a carbonate sand. Soils and Foundations, 61(6), 1708-1717.

14. Gibo, S., Egashira, K., Ohtsubo, M., Nakamura, S., 2002. Strength recovery from residual state in reactivated landslides. Géotechnique 52(9), 683-686.

15. Huang, D., Gu, D.M., Song, Y.X., Cen, D.F. and Zeng, B., 2018. Towards a complete understanding of the triggering mechanism of a large reactivated landslide in the Three Gorges Reservoir. Eng. Geol. 238, 36-51.

16. Kilburn, C.R.J., Petley, D.N., 2003. Forecasting giant, catastrophic slope collapse: lessons from Vajont, Northern Italy. Geomorphology 54 (1), 21–32.

17. Kundu, P., Gupta, N., 2022. Impact of Residual Strength of Soil in Reactivated Landslide: Case Studies of a Few Landslides in Different Regions of the Globe. In Earthquake Geotechnics, 249-258.

18. Lemos, L.J.L., 2003. Shear behaviour of pre-existing shear zones under fast loading—insights on the landslide motion. In Proc. International workshop on occurrence and mechanisms of flow-like landslide motion, 229-236.

19. Lupini, J.F., Skinner, A.E., Vaughan, P.R., 1981. The drained residual strength of cohesive soils. Géotechnique 31(2), 181-213.

20. Liao, K., Wu, Y., Miao, F., 2022. System reliability analysis of landslides subjected to fluctuation of reservoir water level: a case study in the Three Gorges Reservoir area, China. Bull. Eng. Geol. Environ., 81(6), 1-12.

21. Li, C., Fu, Z., Wang, Y., Tang, H., Yan, J., Gong, W., Yao, W., Criss, R.E., 2019. Susceptibility of reservoir-induced landslides and strategies for increasing the slope stability in the Three Gorges Reservoir Area: Zigui Basin as an example. Eng. Geol. 261, 105279.

22. Li, D., Yin, K., Glade, T., Leo, C., 2017. Effect of over-consolidation and shear rate on the residual strength of soils of silty sand in the Three Gorges Reservoir. Scientific reports 7(1), 1-11.

23. Miao, H.B., Wang, G.H., Yin, K.L., Kamai, T., Li, Y.Y., 2014. Mechanism of the slow-moving landslides in Jurassic red-strata in the three Gorges reservoir, China. Eng. Geol. 171 (13), 59–69.

24. Ramiah, B.K., Purushothamaraj, P., Tavane, N.G., 1973. Thixotropic effects on residual strength of remoulded clays. Indian Geotech. J. 3(3), 189-197.

25. Ren, S., Zhang, Y., Xu, N., Wu, R., Liu, X., Du, G., 2021. Mobilized strength of gravelly sliding zone soil in reactivated landslide: a case study of a giant landslide in the north-eastern margin of Tibet Plateau. Environmental Earth Sciences, 80(12), 1-15.
26. Sanshao, R., Yongshuang, Z., Nengxiong, X., Ruian, W., Liu, X., Guoliang, D., 2021. Mobilized strength of gravelly sliding zone soil in reactivated landslide: a case study of a giant landslide in the north-eastern margin of Tibet Plateau. Environmental Earth Sciences, 80(12).
27. Serafim, J.L., 1987. Malpasset Dam discussion — Remembrances of failures of dams. Eng. Geol. 24 (1), 355–366.
28. Schofield, A.N., 2006. Interlocking, and peak and design strengths. Géotechnique 56(5), 357-358.
29. Skempton, A.W., 1970. First time slides in overconsolidated clays. Géotechnique 20 (3), 320–324.
30. Skempton, A.W., 1985. Residual strength of clays in landslides, folded strata and the laboratory. Géotechnique 35(1), 3-18.
31. Song, K., Wang, F.W., Yi, Q.L., Lu, S.Q., 2018. Landslide deformation behavior influenced by water level fluctuations of the Three Gorges Reservoir (China). Eng. Geol. 247, 58–68.
32. Stark, T.D., Choi, H., McCone, S., 2005. Drained shear strength parameters for analysis of landslides. J. Geotech. Geoenviron. 131(5), 575–588.
33. Stark, T.D., Hussain, M., 2010. Shear strength in preexisting landslides. J. Geotech. Geoenviron. 136(7), 957-962.
34. Tang, H.M., Li, C.D., Hu, X.L., Su, A.J., Wang, L.Q., Wu, Y.P., Criss, R., Xiong, C.R., Li, Y., 2015a. Evolution characteristics of the Huangtupo landslide based on in situ tunneling and monitoring. Landslides 12 (3), 511–521.

35. Tang, H.M., Li, C.D., Xiong, C.R., Hu, X.L., Wang, L.Q., Criss, R., Su, A.J., Wu, Y.P., 2015b. Deformation response of the Huangtupo landslide to rainfall and the changing levels of the three Gorges Reservoir. Bull. Eng. Geol. Environ. 74 (3), 933–942.
36. Tang, H. M, Wasowski, J., Juang, C.H., 2019. Geohazards in the three Gorges Reservoir Area, China – Lessons learned from decades of research. Eng. Geol. 261, 105267.
37. Tan, Q., Tang, H., Fan, L., Xiong, C., Fan, Z., Zhao, M., Li, C., Wang, D., Zou, Z., 2018. In situ triaxial creep test for investigating deformational properties of gravelly sliding zone soil: example of the Huangtupo 1# landslide, China. Landslides 15(12), 2499-2508.
38. Tika, T.E., Vaughan, P.R., Lemos, L.J.L.J., 1996. Fast shearing of pre-existing shear zones in soil. Géotechnique 46(2), 197-233.
39. Townsend, F.C., Gilbert, P.A., 1976. Effects of specimen type on the residual strength of clays and clay shales. Soil specimen preparation for laboratory testing. ASTM STP 599, American Society for Testing and Material, 43–65.
40. Vithana, S.B., Nakamura, S., Kimura, S., Gibo, S., 2012. Effects of overconsolidation ratios on the shear strength of remoulded slip surface soils in ring shear. Eng. Geol. 131, 29-36.
41. Wang, S., Wang, J., Wu, W., Cui, D., Su, A., Xiang, W., 2020. Creep properties of clastic soil in a reactivated slow-moving landslide in the Three Gorges Reservoir Region, China. Eng. Geol. 267, 105493.
42. Wang, T., Yin, K., Li, Y., Guo, Z., Wang, W., 2022. Interpretation of the reactivation of slow-moving landslides based on ring shear tests and monitoring. Natural Hazards, 1-23.

43. Wen, B.P., Aydin, A., Duzgoren-Aydin, N.S., Li, Y.R., Chen, H.Y., Xiao, S.D., 2007. Residual strength of slip zones of large landslides in the Three Gorges area, China. Eng. Geol. 93(3-4), 82-98.
44. Zhou, C., Cao, Y., Yin, K., Intrieri, E., Catani, F., Wu, L., 2022. Characteristic comparison of seepage-driven and buoyancy-driven landslides in Three Gorges Reservoir area, China. Eng. Geol. 301, 106590.

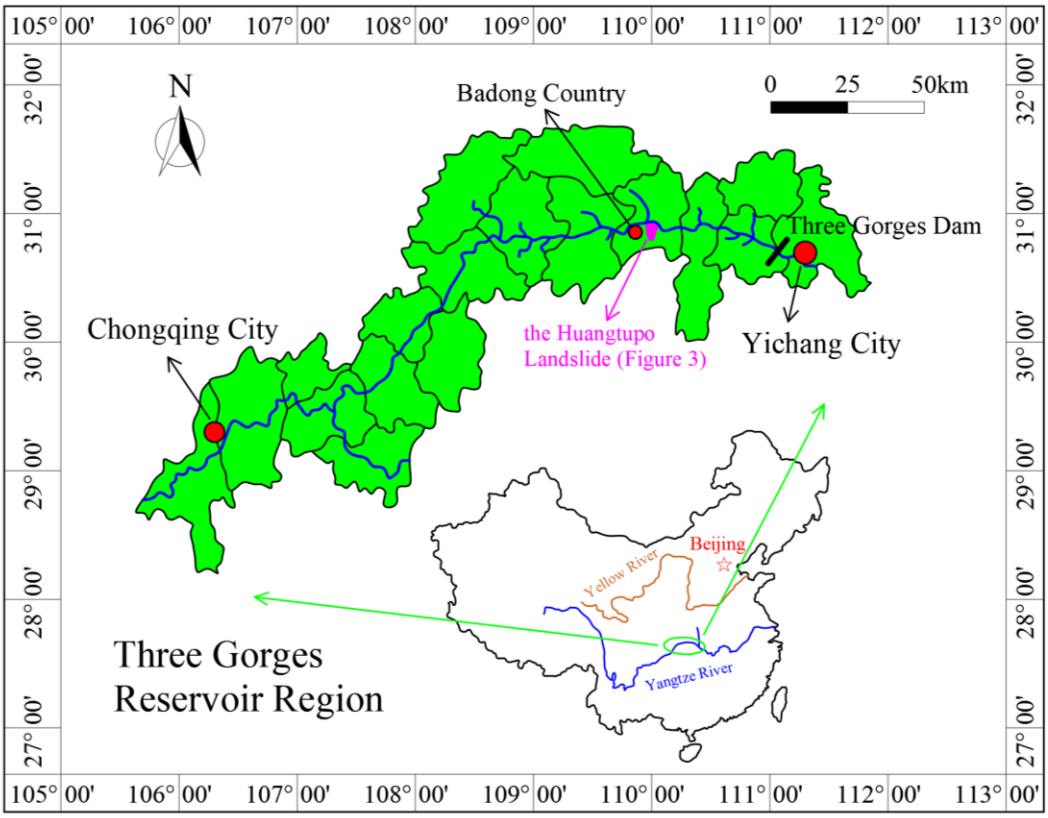

Fig. 1. Location of the Three Gorges Reservoir Region in China (green part) and the Huangtupo landslide (pink part). The small green circle on the insert map of China denotes the Three Gorges Reservoir Region.

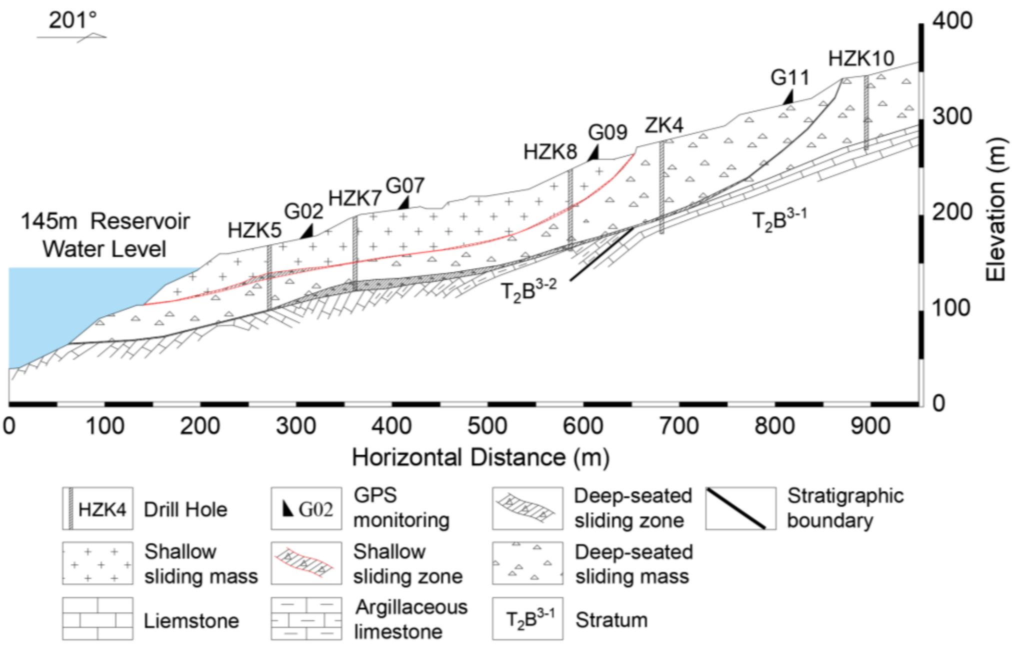

Fig. 2. Geological profile (Section I-I′ in Fig.3) of the Hunagtupo 1# landslide (where $T_2B^{3\text{-}1}$ and $T_2B^{3\text{-}2}$ belong to T_2B_3 stratum).

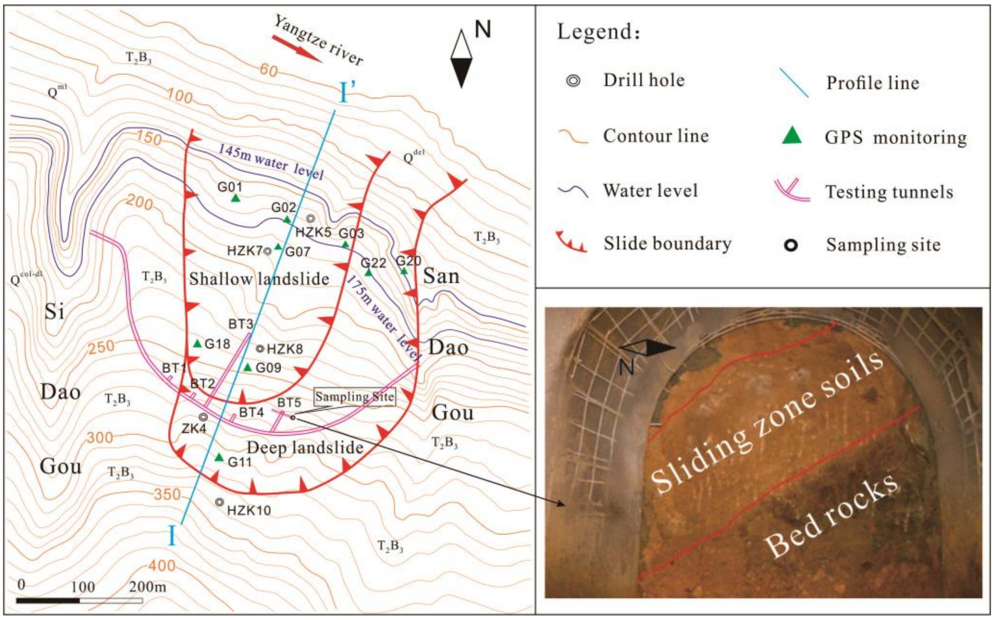

Fig. 3. Landform of the Hunagtupo 1# landslide including some marks of typical vertical sections, and the sampling site of deep-seated sliding zone soil.

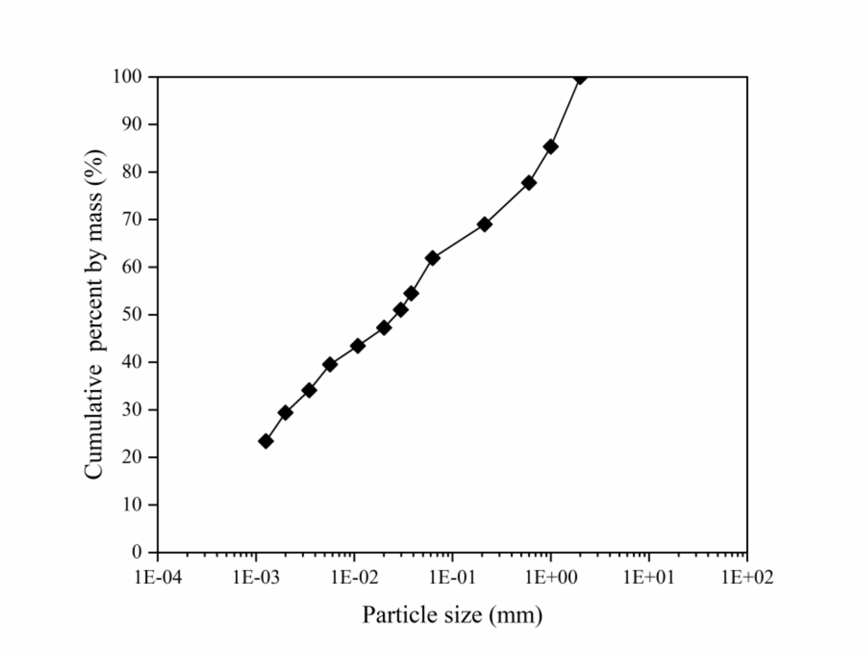

Fig. 4. Grain size distribution of the tested soil sample.

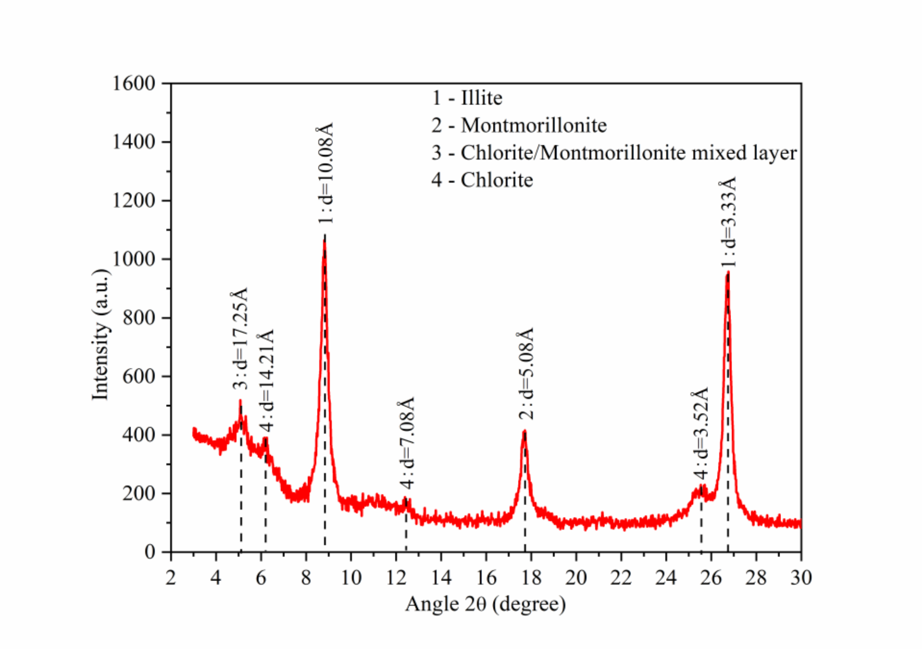

Fig. 5. X-ray diffraction pattern of the clay fraction (< 0.002 mm) of the tested soil.

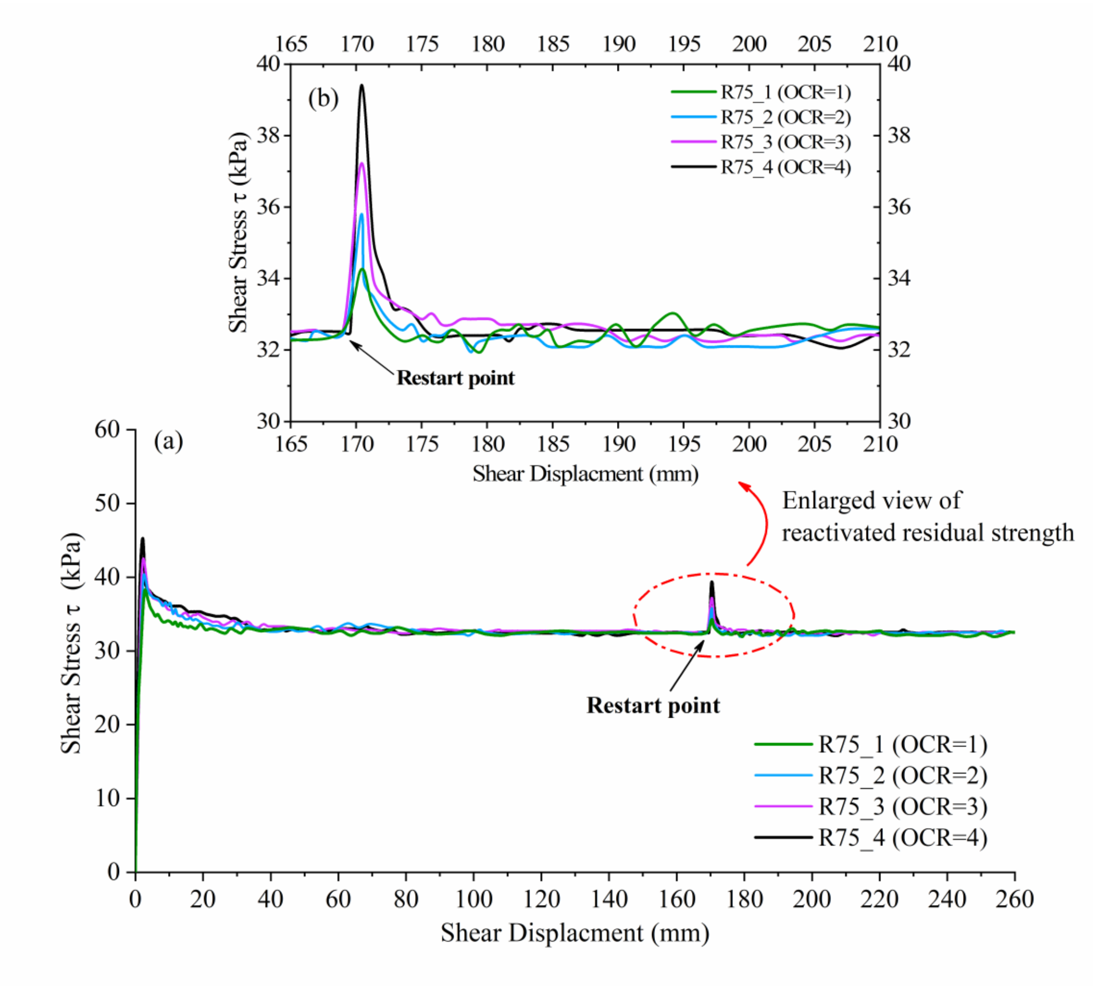

Fig. 6. (a) Results of the reactivation tests under a normal effective stress of 75 kPa; (b) Enlarged view of reactivated residual strength.

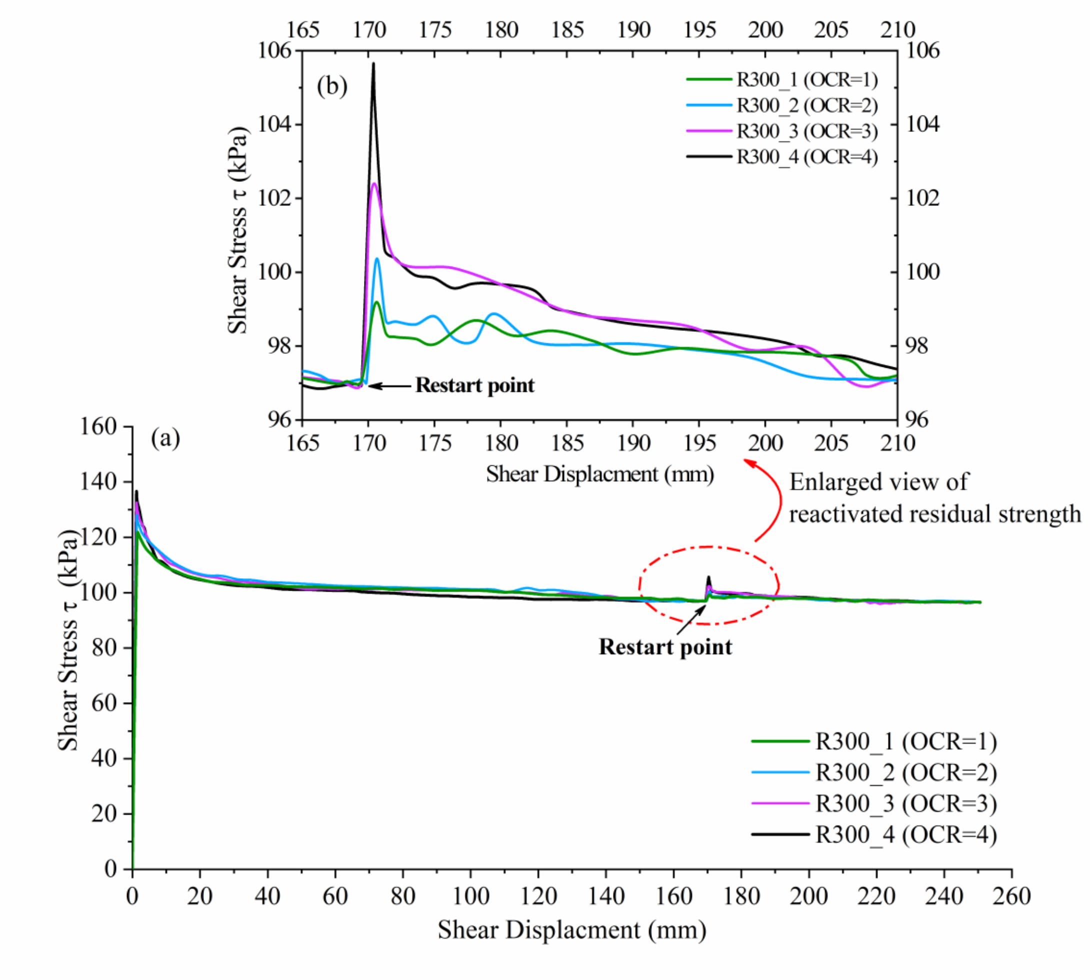

Fig. 7. (a) Results of the reactivation tests under a normal effective stress of 300 kPa; (b) Enlarged view of reactivated residual strength.

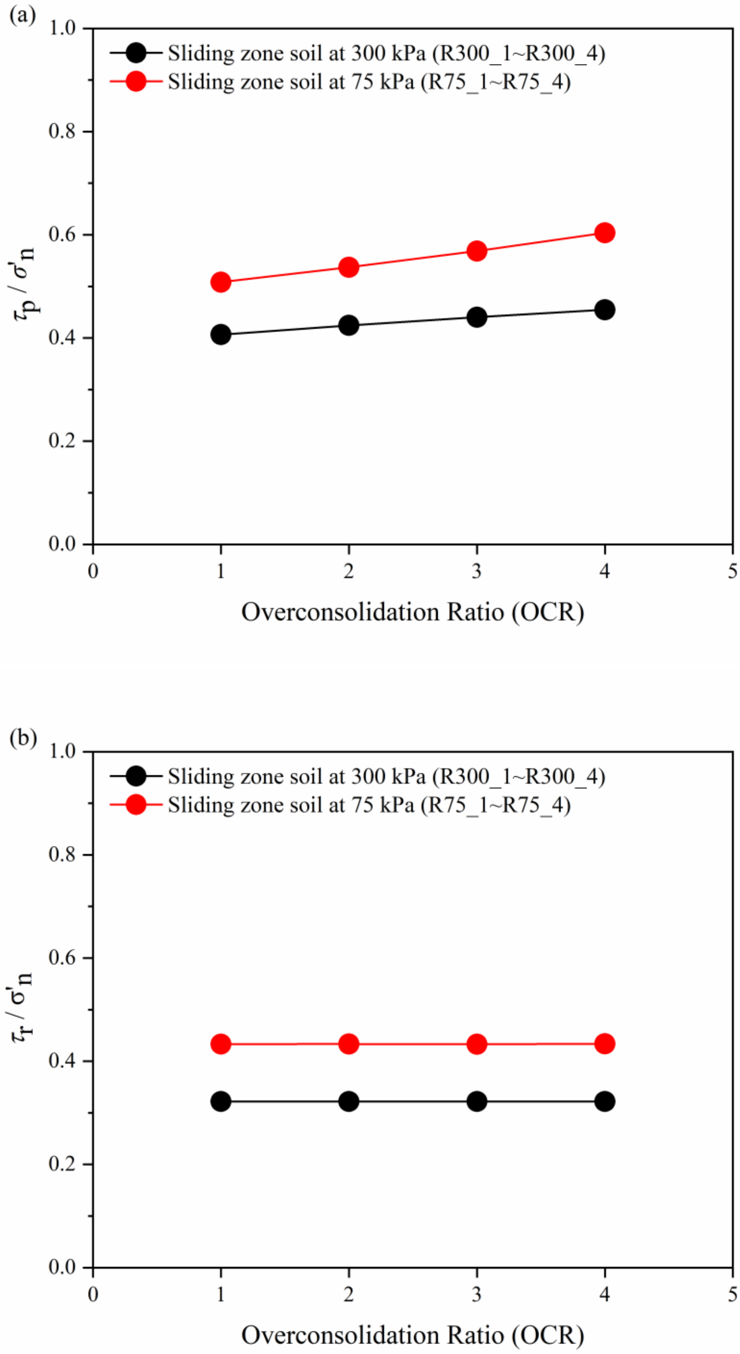

Fig. 8. Relationships between the stress ratio (a) at the peak state and (b) at the residual state and OCR under two different normal effective stresses of 75 kPa and 300kPa.

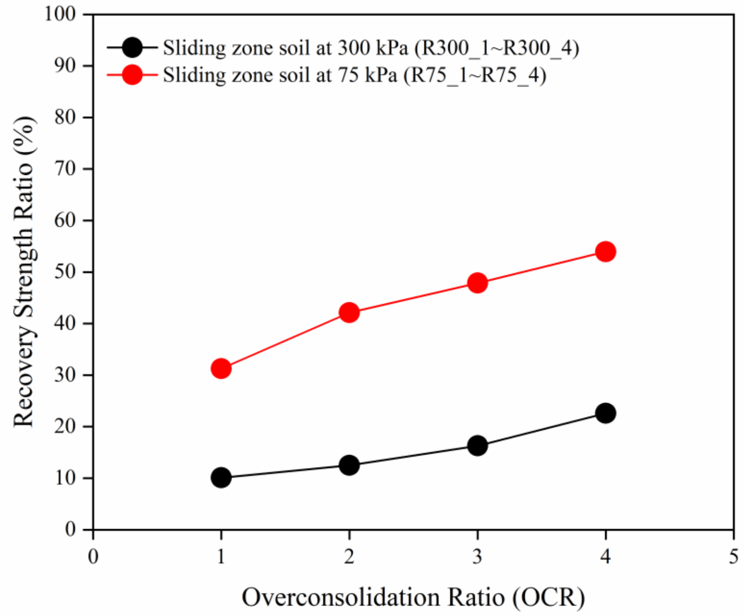

Fig. 9. RSR as a function of OCR under two different normal effective stresses of 75 kPa and 300kPa.

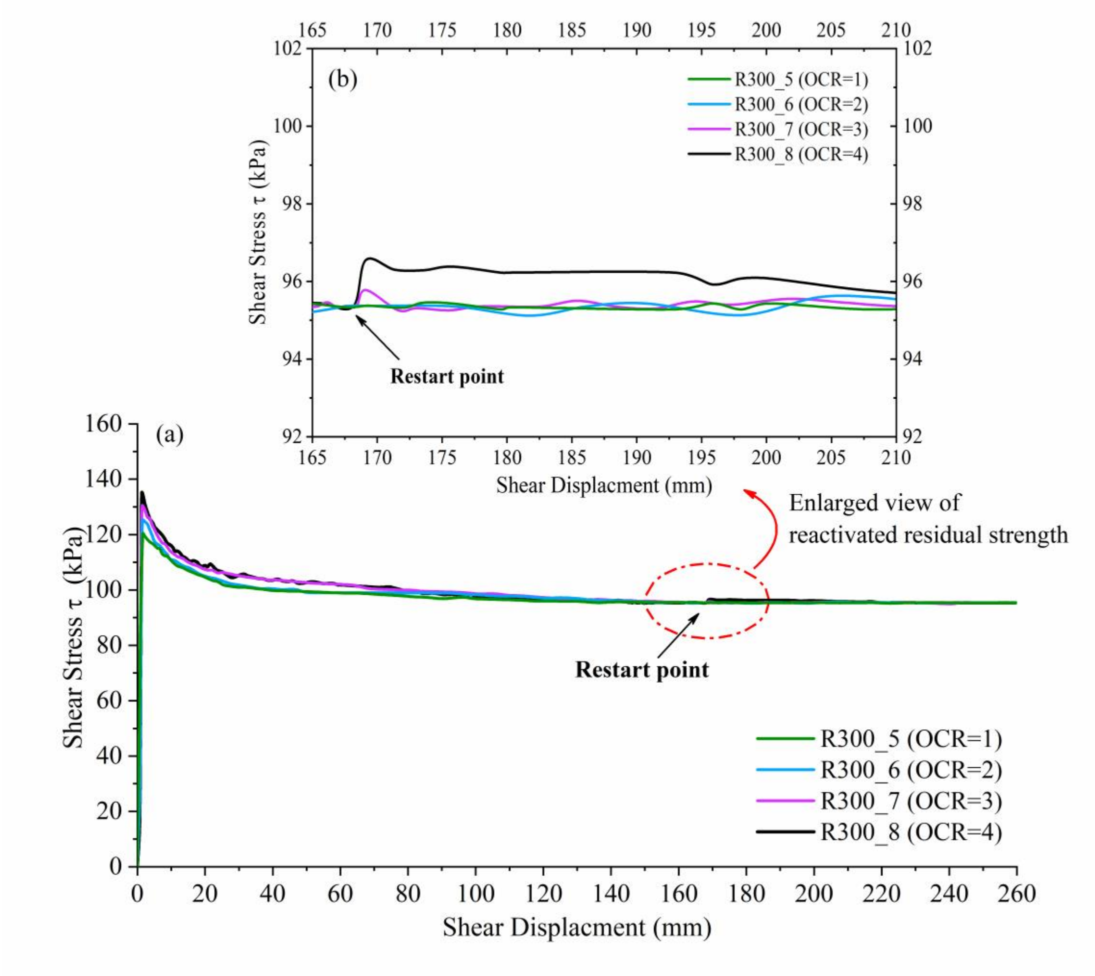

Fig. 10. (a) Results of the reactivation tests on the soil samples with the particle size smaller than 1 mm under a normal effective stress of 300 kPa; (b) Enlarged view of reactivated residual strength.

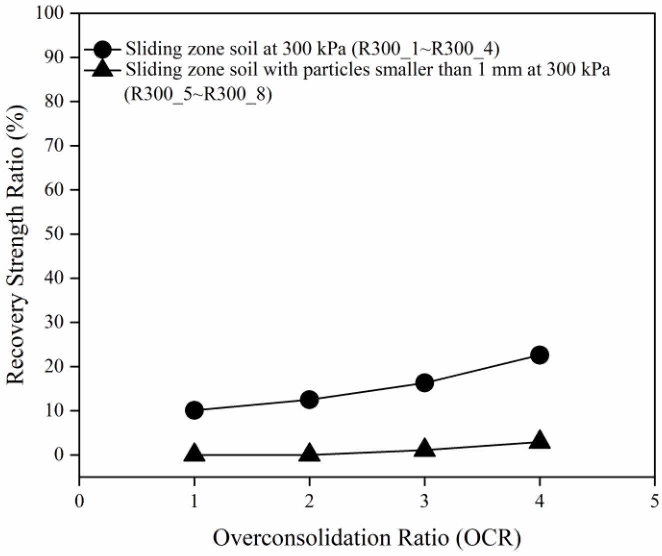

Fig. 11. RSR as a function of OCR for the soil samples with the particle size smaller than 1 mm under a normal effective stress of 300 kPa.

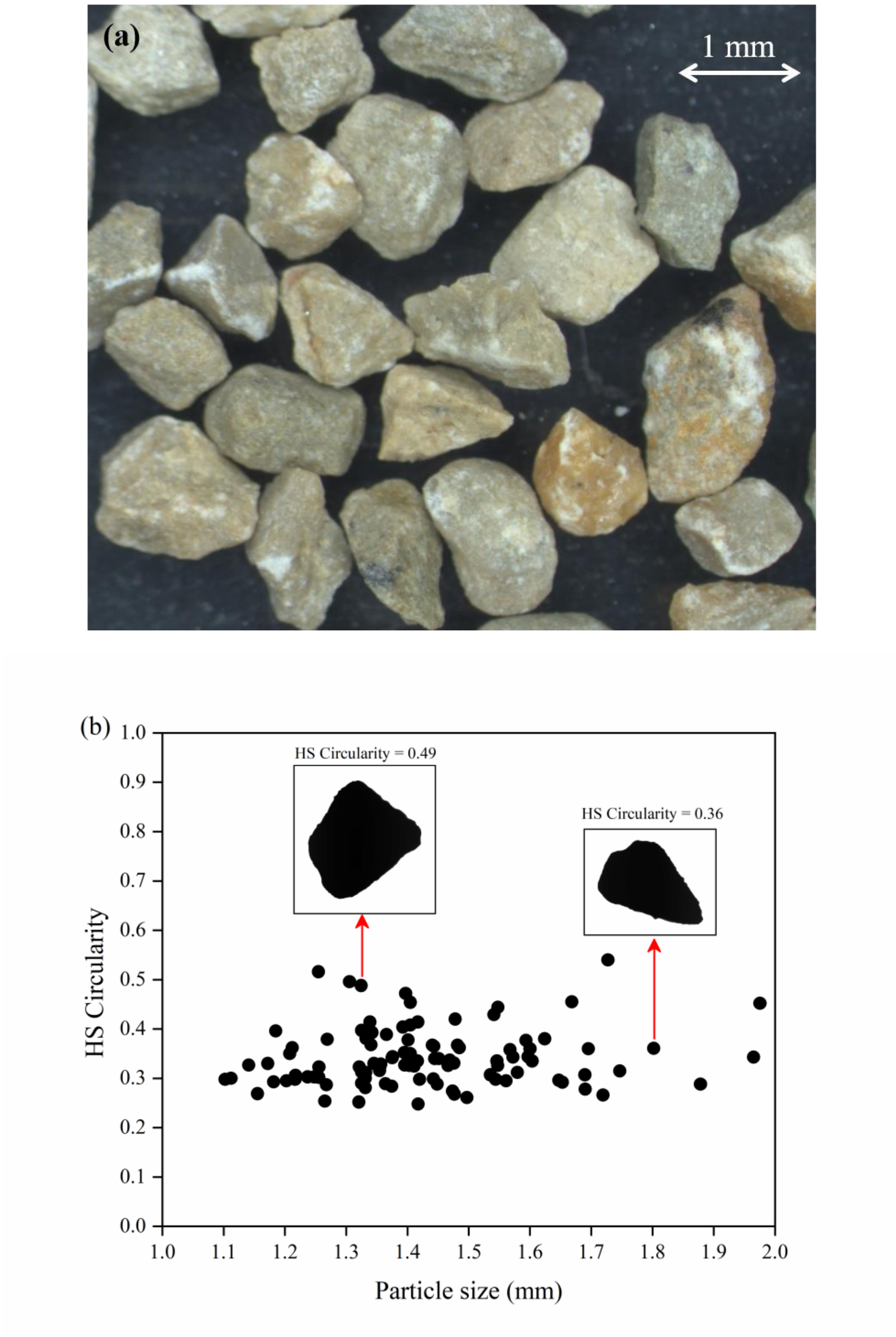

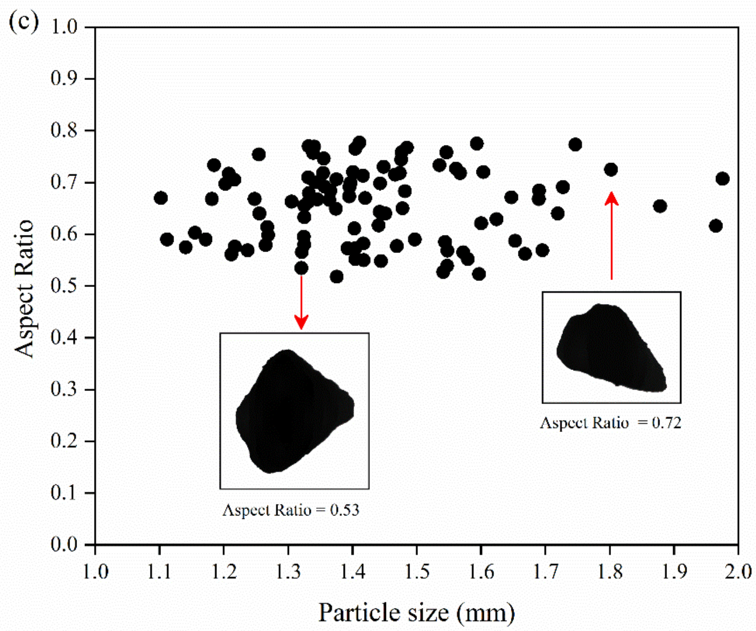

Fig.12. (a) Images of the very coarse sand with a size of 1-2 mm inside the remoulded soil sample, and (b) HS Circularity and (c) Aspect Ratio distributions of 100 very coarse sand particles, obtained by a Morphologi G3 particle analyzer.

Table 1. Geotechnical index properties of the tested soil.

Property	Value
Specific gravity	2.72
Dry density (kg/m^3)	1890
Saturated unit weight (kN/m^3)	22.8
Liquid limit (%)	30.4
Plastic limit (%)	12.8
Plasticity index	17.6
Grain size distribution *	
Sand 0.063 – 2 mm (%)	37.1
Silt 0.002 – 0.063 mm (%)	33.5
Clay < 0.002 mm (%)	29.4

**The British Soil Classification System (BSCS) is used for soil classification in the study.*

Table 2. X-ray diffraction analysis of the tested soil.

	Non-clay minerals				Clay minerals			
	Quartz	Calcite	Plagioclase	Orthoclase	Montmorillonite	Illite	Chlorite/ Montmorillonite *	Chlorite
Content (%)	21.4	25.9	1.5	1.1	7.3	31.2	6.2 (71.4)	5.4

**the Montmorillonite content, as %, in the Cholrite/ Montmorillonite mixed-layer is specified in brackets*

Table 3. Details of reactivation tests.

Test	Coarse sand content (1-2 mm) (%)	Consolidation stress (kPa)	Normal effective stress σ'_n (kPa)	OCR	Shear displacement before resting (mm)	Shear rate (mm/min)	Rest time
R300_1	14.8	300	300	1	170.4	0.1	24 h
R300_2		600	300	2			
R300_3		900	300	3			
R300_4		1200	300	4			
R300_5	0	300	300	1	170.4	0.1	24 h
R300_6		600	300	2			
R300_7		900	300	3			
R300_8		1200	300	4			
R75_1	14.8	75	75	1	169.1	0.1	24 h
R75_2		150	75	2			
R75_3		225	75	3			
R75_4		300	75	4			

Table 4. Test data of the reactivation tests under different experimental conditions.

Test	Peak strength τ_p (kPa)	Residual strength τ_r (kPa)	Reactivated residual strength τ_{rea} (kPa)	Strength recovery τ_{rea} - τ_r (kPa)	RSR (%)
R300_1	122.0	96.6	99.2	2.6	10.1
R300_2	127.3	96.6	100.4	3.8	12.5
R300_3	132.1	96.6	102.3	5.8	16.3
R300_4	136.5	96.6	105.6	9.0	22.6
R75_1	38.1	32.5	34.3	1.8	31.3
R75_2	40.3	32.5	35.8	3.3	42.1
R75_3	42.6	32.5	37.4	4.9	48.2
R75_4	45.3	32.5	39.5	6.9	53.9
R300_5	120.3	95.4	95.4	0	0
R300_6	125.1	95.4	95.4	0	0
R300_7	130.4	95.4	95.8	0.4	1.1
R300_8	134.8	95.4	96.5	1.1	2.9